IEEE Access
Multidisciplinary : Rapid Review : Open Access Journal

Received June 10, 2020, accepted July 6, 2020, date of publication July 16, 2020, date of current version July 28, 2020.

Digital Object Identifier 10.1109/ACCESS.2020.3009668

A Modified INC Method for PV String Under Uniform Irradiance and Partially Shaded Conditions

LIBIN XU, RUOFA CHENG, AND JIAJING YANG
School of Information Engineering, Nanchang Hangkong University, Nanchang 330063, China

Corresponding author: Ruofa Cheng (rfcheng36@126.com)

This work was supported in part by the National Natural Science Foundation of China under Grant 51567019, and in part by the Science and Technology Support Program of Jiangxi Province, China, under Grant 20142BBE50002.

ABSTRACT Due to the bypass diodes, the partially shaded photovoltaic (PV) string exhibits multiple peaks in the *P-V* curve. And the conventional Maximum Power Point Tracking (MPPT) methods are not capable of tracking the global peak (GP) under partially shaded condition (PSC). In order to track the GP fast and efficiently under uniform irradiance condition (UIC) and PSC, a modified incremental conductance (INC) method is proposed in this paper. This method can not only detect the occurrence of PSC, but also determine if the other peaks need to be tracked under PSC by using the relationship between the minimum current at other peaks and the short circuit current to enhance the tracking speed. In order to improve efficiency, the converter duty cycle will be regulated slightly to ensure that the operating point reaches in the vicinity of GP, after the approximate GP is located. The Matlab simulation results show that the proposed method is faster and more efficient than other methods. It only requires 3 and 11 sampling cycles to locate the GP under UIC and PSC, respectively. Its overall tracking efficiency is increased by 13.61%, 4.28% and 0.42% under UIC, PSC and one-day irradiance profile respectively, compared to the conventional INC method.

INDEX TERMS PV string, maximum power point tracking (MPPT), global peak (GP), uniform irradiance condition (UIC), partially shaded condition (PSC).

I. INTRODUCTION

The MPPT methods, including the conventional and advanced methods, are proposed to track the MPP. Because there is only one peak (i.e. MPP) under UIC, the conventional MPPT algorithms such as INC [1]–[4], perturb and observe (P&O) [5]–[7] can track the MPP successfully. However, they are not capable of tracking the GP under PSC, due to the multi-peak characteristic of partially shaded PV system [8], [9]. The advanced methods such as neural network [10]–[12] and evolutionary computation [13]–[18] are better than the conventional algorithms under both UIC and PSC. But the advanced algorithms have more complex structure, and they are more difficult to implement, compared to the conventional MPPT methods.

A few modified algorithms based on the conventional MPPT methods have been introduced to track the GP under PSC. Patel and Agarwal [19] have introduced a novel MPPT method that uses the characteristic of GP on *P-V* curve and a feedforward control scheme to track the GP under PSC. But it needs to search the entire voltage range, which leads to large power oscillations and losses. Chen *et al.* [20] have presented an improved P&O that is able to distinguish between the GP and local peak (LP). It requires some voltage sensors to calculate the number of MPPs and detect the occurrence of PSC, and this method has good performance under PSC. Tey and Mekhilef [21] have designed a modified INC that uses the characteristic of GP introduced in [19] and the relationship between the load line and *I-V* curve to track the GP under PSC. However, in the case of UIC, the entire voltage space needs to be explored, causing low tracking speed. That is because this method is not capable of distinguishing between the irradiance variation under UIC and the occurrence of PSC. Ahmed and Salam [22] have proposed an enhanced adaptive P&O (EA-P&O). In EA-P&O, the PSC is determined by using the irradiance level at

The associate editor coordinating the review of this manuscript and approving it for publication was Giambattista Gruosso.

This work is licensed under a Creative Commons Attribution 4.0 License. For more information, see https://creativecommons.org/licenses/by/4.0/

the MPP and short circuit current position, and the GP can be tracked successfully. Ghasemi *et al.* [23] come up with a novel two-stage MPPT method, which includes the method to determine the occurrence of PSC and a new algorithm to track the GP. The advanced MPPT methods based on neural network or evolutionary computation have been put forward. Manickam *et al.* [24] have proposed a hybrid algorithm by combining P&O and particle swarm optimization (PSO), which performs P&O and PSO under UIC case and PSC case, respectively. The drawback of this method is that if the PSC detection fails, this algorithm will never shift to PSO [25]. Mohanty *et al.* [26] have presented a hybrid MPPT algorithm that combines grey wolf optimization (GWO) with P&O to overcome the problem of low tracking efficiency and steady state oscillation. Zhang *et al.* [27] have introduced a hybird MPPT method, which combines artificial neural network (ANN) and modified P&O (MP&O). This method uses ANN to find GP at the optimal voltage areas fistly, then calls MP&O to locate the GP, and reduces fluctuation by using adaptive step size. Some novel MPPT algorithms have been proposed. Wang *et al.* [28] have introduced the search-skip-judge global MPPT (SSJ-GMPPT) and rapid global MPPT (R-GMPPT). And they can speed up the tracking speed and improve efficiency. Wei *et al.* [29] have proposed a new algorithm, which uses liner equation to calculate the peaks voltage at different peak intervals, and obtain the corresponding peaks power. By comparing these peaks, the GP can be tracked quickly and accurately. Fan *et al.* [30] have designed a qucik MPPT method to locate the GP on one step, by using the mathematical model and the internal parameters.

Most of the above mentioned algorithms are designed for PV string under PSC, not UIC. So, they yield poor tracking performance under UIC. Based on this problem, this paper proposes a modified INC method which can track the GP under both UIC and PSC. This algorithm can not only distinguish between the irradiance variation under UIC and the occurrence of PSC, but also determine whether it is necessary to track the other peaks under PSC to improve the converging speed. After the approximate GP location is determined, the converter duty cycle will be modulated slightly to ensure that the operating point locates in the vicinity of GP, and improve the tracking efficiency.

The rest of the paper is organized as follows. The next section describes the conventional INC algorithm, and shows the characteristics curves of PV string under UIC and PSC. In section III, the proposed method tracking under UIC and PSC is introduced. Section IV presents the simulation results and evaluations under various conditions, such as UIC case, PSC case and one-day irradiance case. Finally, the conclusion of this paper is highlighted in section V.

II. REVIEW OF THE CONVENTIONAL INC

Since INC and P&O methods can be implemented easily, they are more commonly used than other MPPT algorithms. The conventional INC algorithm modulates the converter duty cycle according to the slope of *P*-*V* curve ($\frac{dP}{dV}$), as presented

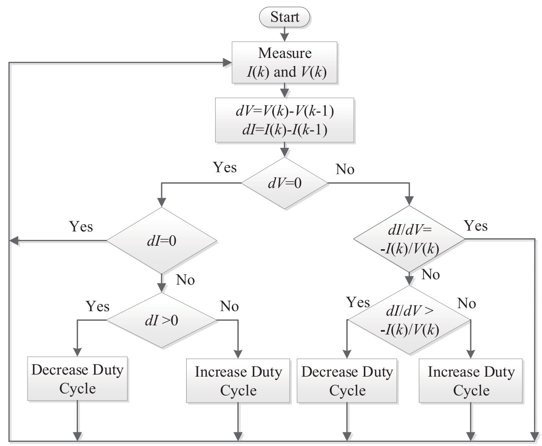

FIGURE 1. Flowchart for the conventional INC algorithm.

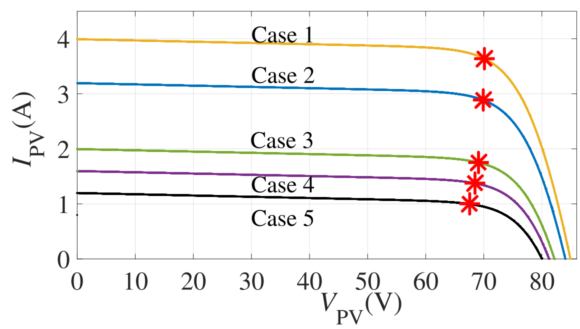

(a) $I-V$ curves

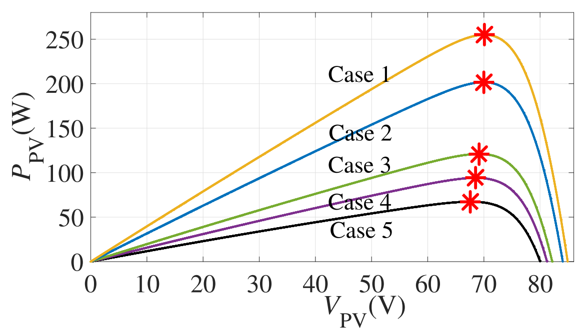

(b) $P-V$ curves

FIGURE 2. Characteristics curves of the PV string under UIC.

in Fig.1. When $\frac{dP}{dV}=0$, the duty cycle will be kept fixed. If $\frac{dP}{dV}>0$, it means that the operating point is at the left of peak, and the duty cycle will be decreased. Otherwise, the duty cycle will be increased.

When the PV string made up of four PV modules in series operates under UIC (cases 1 to 5 in Table 1), its characteristics curves only have one peak, as shown in Fig.2. So, the conventional INC method can track the MPP successfully. Under PSC (cases 6 to 10), the multiple peaks are existed on characterics curves, as presented in Fig.3. The peak located by INC method may be LP, and INC is unable to distinguish between GP and LP. Once the tracked peak is LP, it will result

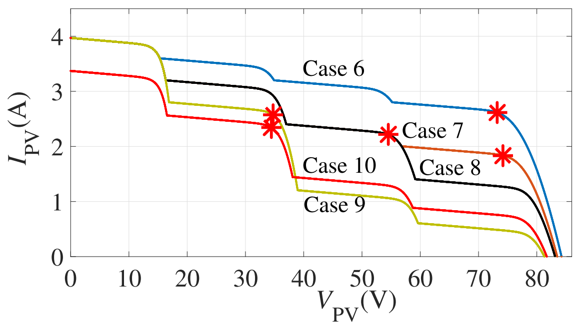

(a) $I-V$ curves

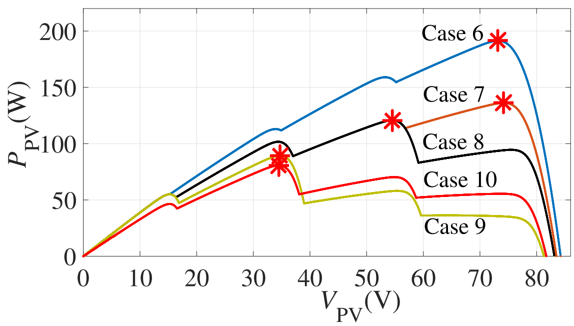

(b) $P-V$ curves

FIGURE 3. **Characteristics curves of the PV string under PSC.**

TABLE 1. **Irradiance levels of the PV modules in PV string.**

Case	Irradiance level (W/m^2)			
	Module 1	Module 2	Module 3	Module 4
1	1000	1000	1000	1000
2	800	800	800	800
3	500	500	500	500
4	400	400	400	400
5	300	300	300	300
6	700	800	900	1000
7	500	600	800	1000
8	350	600	800	1000
9	150	300	700	1000
10	220	360	640	850

in low tracking efficiency. Hence, it is vital to track the GP under both UIC and PSC.

III. THE PROPOSED MODIFIED INC

DC-DC converters such as boost, buck, sepic and buck-boost are applied in the PV system. Although the structure of boost and buck converters is simple, they have a non-operational region [32]. While buck-boost and sepic converters can be seen as the ideal MPPT applications [32]. Thus, the buck-boost converter is utilized in this paper. When this converter operates in continuous inductor current mode, the relation between input and ouput can be described as follows [33]:

$$V_{out} = V_{PV} M_{(D)} \tag{1}$$

$$I_{out} = \frac{I_{PV}}{M_{(D)}} \tag{2}$$

where V_{out} and I_{out} are the ouput voltage and current, respectively. V_{PV} and I_{PV} refer to PV voltage and current, respectively. $M_{(D)} = \frac{-D}{1-D}$, and D denotes the converter duty cycle.

Dividing (1) by (2), yields

$$\frac{V_{out}}{I_{out}} = \frac{M_{(D)}^2 V_{PV}}{I_{PV}} \tag{3}$$

or

$$R_{load} = M_{(D)}^2 R_{eq} \tag{4}$$

where $R_{load} = \frac{V_{out}}{I_{out}}$, which represents the load resistance; $R_{eq} = \frac{V_{PV}}{I_{PV}}$, that is the input resistance.

If the converter duty cycle D is known, R_{load} can be computed, according to (4). And the new duty cycle D_{new} can be calculated as the following equation [34]:

$$D_{new} = \frac{\sqrt{a}}{1+\sqrt{a}} \tag{5}$$

where, $a = \frac{I_{PV}}{V_{PV}} R_{load}$.

In order to locate the GP successfully under both UIC and PSC, a modified INC method is proposed in this paper. Fig.4 shows the concept diagram, which includes four blocks, such as PV data measure block, power deviation checking block, load and irradiance variation detection block, and MPPT controller block. The detailed flowchart of the proposed method is presented in Fig.5.

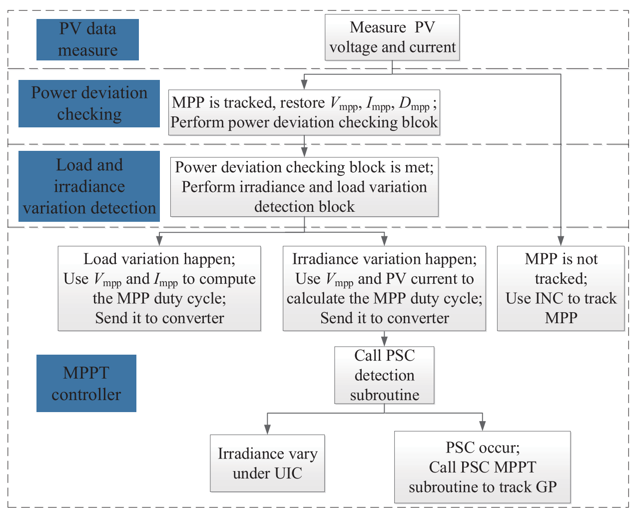

FIGURE 4. **Concept diagram for the proposed algorithm.**

A. TRACKING UNDER UIC

Due to the steady state oscillation, the conventional INC method has power losses. To eliminate oscillation at the steady state, an error can be used, as shown as [2]:

$$\left|\frac{I}{V} + \frac{\Delta I}{\Delta V}\right| < 0.07 \tag{6}$$

And (6) also can be used to judge whether the approximate GP location is found. To improve efficiency, when (6) is met,

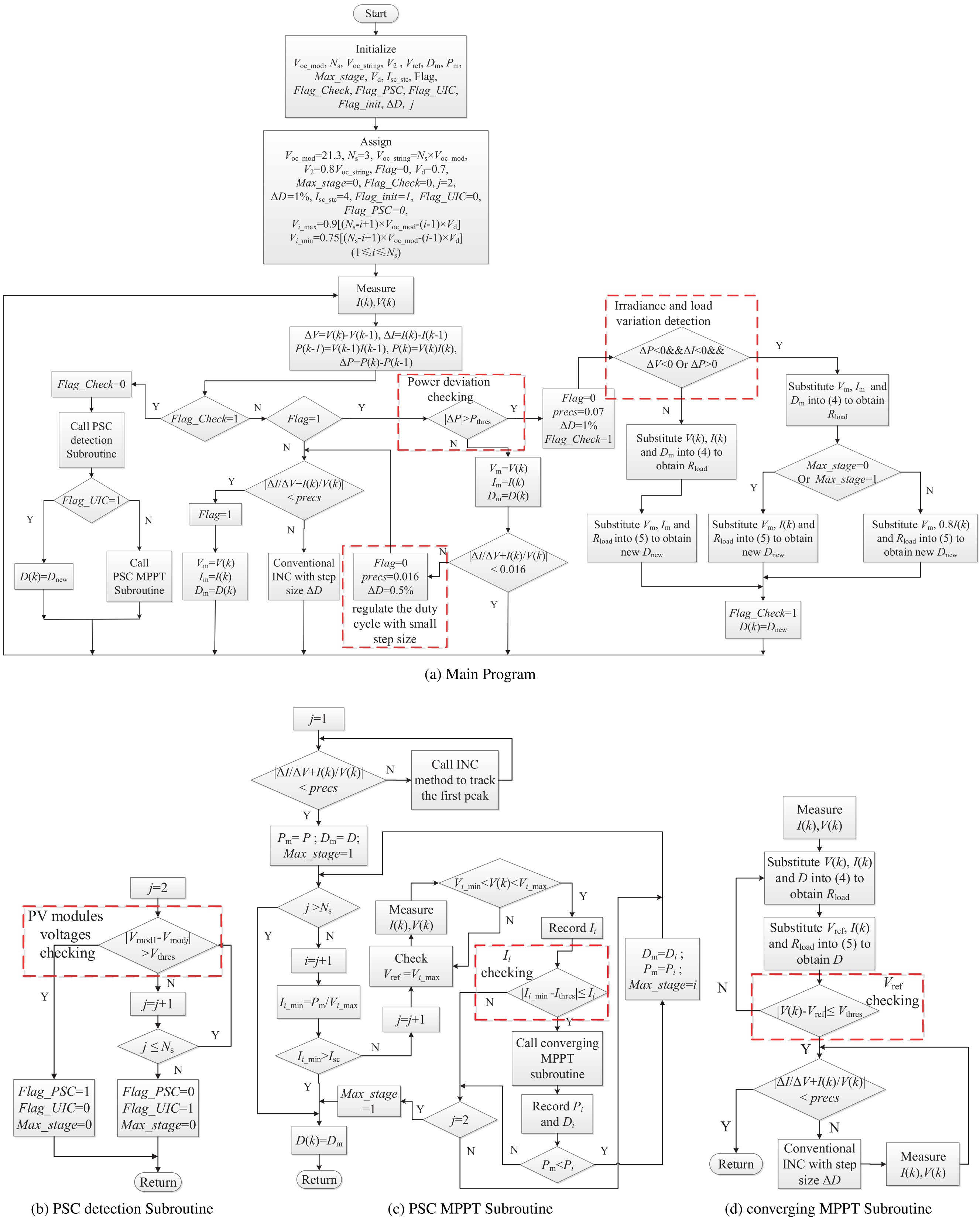

FIGURE 5. Flowchart for the proposed algorithm.

(7) will be used to ensure that the operating point comes in the vicinity of GP, as shown in below:

$$|\frac{I}{V} + \frac{\Delta I}{\Delta V}| < 0.016 \quad (7)$$

Assmuing that the PV string operates under UIC, the modified INC method calls the conventional INC algorithm to regulate duty cycle firstly. Then the proposed method needs to check whether (6) and (7) are satisfied. If both (6) and (7) are not met, the duty cycle step size ΔD is 1%. Otherwise, ΔD is decreased to 0.5%, as shown in Fig.5(a). When (6) is satisfied, *Flag* is changed to 1, it means that the peak (i.e. MPP) is tracked. The voltage, current and duty cycle are recorded. Then, the proposed method will check if the absolute value of power difference $|\Delta P|$ is larger than P_{thres} at the next sampling cycle. When the power deviation checking block is not met, if (7) is not met, *Flag* becomes 0, the converter duty cycle D is modulated with 0.5%, and it can improve the tracking efficiency; otherwise, the duty cycle remains unchanged.

When $|\Delta P|$ is largger than P_{thres}, it indicates that irradiance or load changes suddenly. It is necessary to determine the cause of the power deviation by using the voltage difference ΔV, current difference ΔI and power difference ΔP, as presented in Table 2 [35].

TABLE 2. The relation between ΔV, ΔI, ΔP and the change of load or irradiance.

	Load		Irradiance	
	increase	decrease	increase	decrease
ΔV	positive	negative	positive	negative
ΔI	negative	positive	positive	negative
ΔP	negative	negative	positive	negative

If the condition (irradiance and load variation detection block) is not met, it means that the change of load resistance occurs; otherwise, the irradiance changes. When the variation of load occurs, it is important to note that the characteristics curves are unchanged. The PV voltage, current and D_m are used to obtain R_{load}. Then, V_m, I_m and R_{load} are substituted into (5) to yield the new duty cycle. When the irradiance changes, the irradiance and load variation detection block is satisfied. In this work, the load and irradiance does not change simultaneously, so the load resistance R_{load} can be caculated by using V_m, I_m and D_m. Then, it is necessary to check which peak such as the first peak (rightmost peak), and third peak, is tracked by the proposed algorithm before the power deviation happens. If the located peak is the first peak (i.e. $Max\_stage = 0$ or 1), the PV current, V_m and R_{load} are substituted into (5) to obtain new duty cycle. Otherwise, using 0.8 times the PV current, V_m and R_{load} to compute the new duty cycle.

After caculating the new duty cycle D_{new}, the conveter duty cycle is switched to it, the variable *Flag_Check* is set to 1. At the next sampling cycle, the PSC detection subroutine will be called. According to the voltages of the PV modules are different under PSC [20], so the PSC detection subroutine uses voltages to detect the occurence of PSC. If the PV modules voltages checking block is not satisfied, it means that PV system operates under UIC, *Flag_UIC* and duty cycle are changed to 1 and D_{new}, respectively. Otherwise, PV string operates under PSC, *Flag_PSC* is switched to 1, and the PSC MPPT subroutine is called.

B. TRACKING UNDER PSC

When PV string operates under PSC, due to the different voltage on each module, the PV modules voltages checking block in the PSC detection subroutine is satisfied. After this subroutine is performed, the proposed method calls the PSC MPPT subroutine, as shown in Fig.5. The first peak (rightmost peak) can be tracked by the conventional INC method. When (6) is met, the proposed method saves the corresponding power and duty cycle as P_m and D_m, respectively. And *Max_stage* is set to 1, which means that the GP is positioned at the first peak. The minimum current at the i^{th} peak will be calculated in the next step, as represented as follow:

$$I_{i\_min} = \frac{P_m}{V_{i\_max}} \quad (1 < i \leq N_s) \quad (8)$$

where the variable N_s is the number of PV modules in series. V_{i_max} refers to the upper voltage limit at the i^{th} peak. The upper and lower voltage limit can be computed as the following equations [24]:

$$V_{i\_max} = 0.95[(N_s - i + 1)V_{oc} - (i-1)V_d] \quad (1 < i \leq N_s) \quad (9)$$

$$V_{i\_min} = 0.70[(N_s - i + 1)V_{oc} - (i-1)V_d] \quad (1 < i \leq N_s) \quad (10)$$

where the variable V_d is the forward diode voltage.

If the minimum current at other peaks is higher than the short circuit current I_{sc} under standard testing conditions (STC), it means that the power at other peaks power is less than P_m, and GP has been located. Otherwise, the other peaks power may be higher than P_m, the proposed method will locate the upper voltage limit V_{i_max} until the PV voltage is between the corresponding lower and upper voltage limit, namely V_{i_min} and V_{i_max}, as shown in Fig.5(c). After that, the current is recorded as I_i. If the I_i checking block is not met, it means that the i^{th} peak power is less than P_m. And if j is equal to 2, it indicates that the first peak is GP, such as cases 6 and 7 in Fig.3; otherwise the other peaks must be checked. Otherwise, the I_i checking block is satisfied, which means the i^{th} peak power may be larger than P_m. Then, the converging MPPT subroutine is called to locate the i^{th} peak. In the converging MPPT subroutine, the rapid modulating method introduced in [21] can be used to enhance the converging speed. It is the process that these variables, including R_{load} calculated from (4), the desired value of the voltage and current, are substituted into (5) to obtain the new duty cycle, as presented in Fig.5(d). And this process continues until the difference between PV voltage and V_{ref} is smaller than

V_{thres} (i.e. the V_{ref} checking block is satisfied). When the V_{ref} checking block is met, but (6) not, the converter duty cycle will be regulated with 1%. When the i^{th} peak is tracked, the power and duty cycle are saved as P_i and D_i, respectively. If P_i is greater than P_m, the variables D_m, P_m and Max_stage are updated to D_i, P_i and i respectively, such as cases 8 to 10; otherwise the proposed method checks if j is equal to 2. After the PSC MPPT subroutine is performed, the approximate GP location is found, and the converter duty cycle will be modulated to make both (6) and (7) are satisfied.

IV. RESULTS AND DISCUSSION

In Matlab/Simulimk, the PV system, comprising PV string, controller and buck-boost converter, is builted. The PV string is made up of four modules in series, and the specification of PV module (MSX-64) is given in Table 3 [31]. In the MPPT controller, the sampling time is set as 0.05s. The simulation results under different scenarios, including UIC case (irradiance and load variation), PSC case and one-day case, are analyzed in this section.

TABLE 3. Parameters of PV module MSX-64 under STC.

Item	Specification
Power at MPP, P_{mpp}	64 W
Voltage at MPP, V_{mpp}	17.5 V
Current at MPP, I_{mpp}	3.66 A
Short.circuit.current, I_{sc}	4 A
Open.circuit.voltage, V_{oc}	21.3 V

A. TRACKING UNDER UIC

The conventional INC algorithm and proposed method are carried out under UIC. Their step size and the initial duty cycle both are 1% and 50%, respectively.

1) IRRADIANCE VARIATION CONDITION

Fig.6 presents the simulation results under irradiance variation condition. The solar irradiation is switched from case 4 to case 1 in Table 1 at $t = 1\,s$, and decreased to case 5 at $t = 2\,s$, then increased to case 2 at $t = 3\,s$. From $t = 0\,s$ to $t = 4\,s$, the load resistacne is fixed at 40Ω.

Under case 4, these methods all can track the MPP. From Fig.6, it can be observed that the tracking speed with the proposed method is faster than that of conventional INC method. The conventional INC method requires 0.65s, 0.90s and 0.60s to reach the MPP under cases 1, 5 and 2 respectively. While the proposed method only takes 0.15s, 0.10s and 0.10s respectively. Thus, the tracking speed of proposed method is 6.14 times faster than that of INC algorithm.

The detailed tracking process of the proposed method is shown in Fig.7. When the irradiance level is case 4, the initial duty cycle is 50%. The proposed method takes 0.05s to regulate the duty cycle, and it is decreased to 49%. At $t = 0.05s$, (6) is satisfied, the duty cycle is kept fixed, and the variable *Flag* is set to 1. After 1 sampling cycle, $t = 0.10s$, since (7) is not met, *Flag* is changed to 0, and the step size is decreased

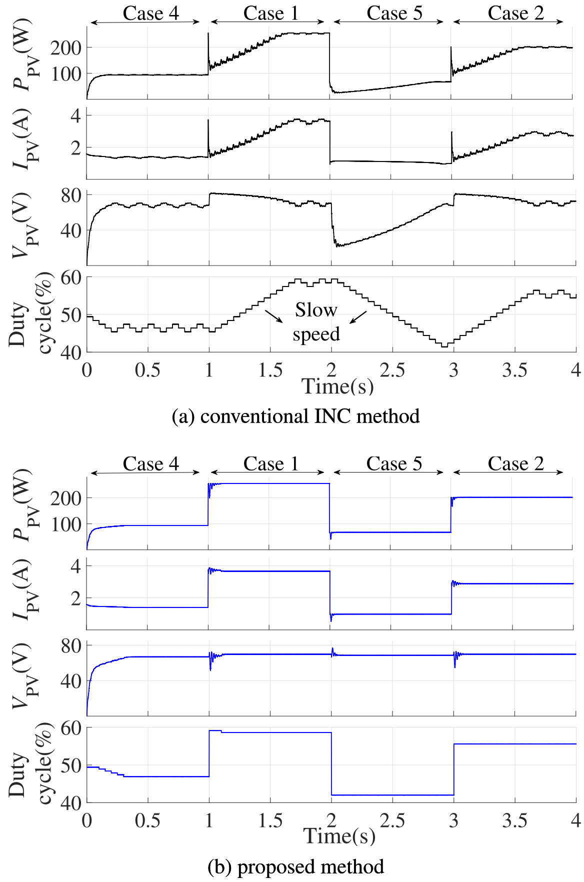

FIGURE 6. Simulation results of conventional INC and proposed algorithm under irradiance variation condition.

from 1% to 0.5%. The process that the duty cycle is regulated with 0.5% needs 5 sampling cycles. At $t = 0.35s$, *Flag* is switched to 1. During this period, the operating point is changed from A_1 to A_2, which comes in the vicinity of the MPP (point A), and the tracked power is obviously increased, as presented in 7(a).

Under case 1, the tracking process is sketched in Fig.7(b). At $t = 1.0\,s$, the solar irradiation is increased from case 4 to case 1. The power difference ΔP is 157W, which is higher than P_{thres}, and it means PV string does not operate at the steady state. Thus, *Flag* is set to 0, the irradiance and load variation detection block is met. Since the variable Max_stage is 0, V_m, PV current and R_{load} obtained from (4) are substituted into (5) to yield the new duty cycle, D_{new}, which is 59.12%, and it will be sent to the converter subsequently. At $t = 1.05\,s$, (6) is met, and *Flag* is changed to 1. However, (7) is not satisfied, and the duty cycle will be regulated with 0.5% at $t = 1.10\,s$. After 1 smapling cycle, *Flag* is switched from 0 to 1.

2) LOAD VARIATION CONDITION

The simulation results for the load variation condition are presented in Fig.8. At $t = 1\,s$, the load resistance is increased from 40Ω to 80Ω. After 40 sampling cycles, $t = 2\,s$, the load

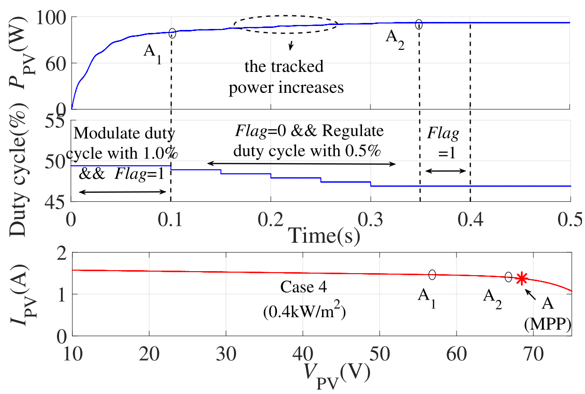

(a) case 4

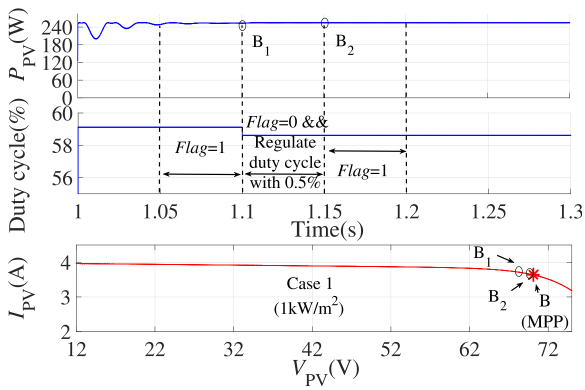

(b) case 1

FIGURE 7. The detailed tracking process of proposed method under cases 4 and 1.

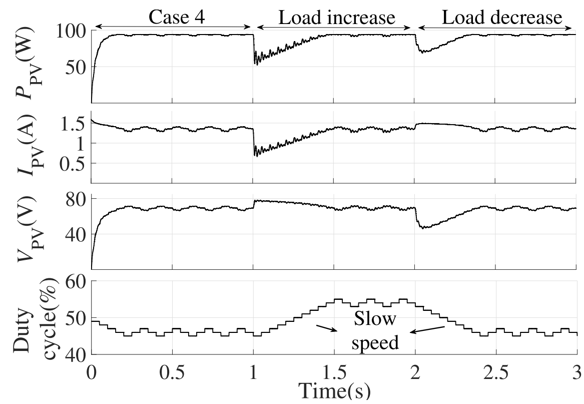

(a) conventional INC method

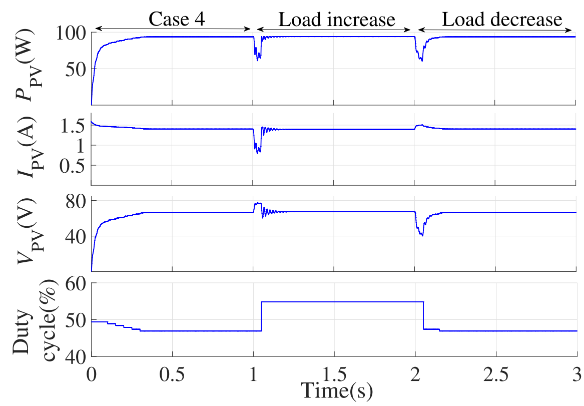

(b) proposed method

FIGURE 8. Simulation results of conventional INC and prosed algorithm under load variation condition.

is decreased back to 40Ω. It is noted that the irradiance level is stayed constant at case 4 from $t = 0\,s$ to $t = 3\,s$.

As can be found from Fig.8, the conventional INC method needs 0.5s and 0.4s to reach the MPP when the load resistance is increased and decreased, respectively. While the proposed method only requires 0.15s and 0.20s, respectively. So, the converging speed of the proposed method is 2.57 times faster than that of INC method.

B. TRACKING UNDER PSC

Under PSC, the proposed method and other methods, such as conventional INC, modified INC (MINC) [21] and EA-INC are carried out, and their step size all are 1%. EA-INC uses the PSC detection and tracking technique described in [22], and it is implemented by INC instead of P&O.

For the efficiency under different PSC conditions, cases 6, 8 and 10 in Table 1 are considered. And they represent that the GP is located at the first, second and third peak respectively. The variations of irradiance in this scenario are as follows: case 4 is imposed for the first 1 s; then, cases 6, 8 and 10 are applied successively for 2 s each.

1) GP AT THE FIRST PEAK

Fig.9 shows the simulation results, and all of MPPT methods can reach the MPP successfully under case 4. At $t = 1\,s$, the irradiance level is switched to case 6, and PSC occurs. As can be observed, these methods all can locate the GP. Among these MPPT methods, the fastest is proposed method with 0.40 s (8 sampling cycles), followed by the conventional INC and EA-INC method(0.50 s and 0.55 s), the slowest is MINC with 0.65 s.

Fig.10 illustrates the detailed tracking process of proposed method under case 6. The proposed method tracks the first peak firstly, and then determines if the other peaks need to be located. Due to the occurence of PSC at $t = 1.0\,s$, the voltages of the PV modules are different. After calling PSC detection subroutine, *Flag_PSC* is set to 1. And the PSC MPPT subroutine is performed subsequently. At $t = 1.05\,s$, (6) is met, that means the first peak is located. The variables P_m and D_m are set to 179.20W and 55.14%, respectively. The operating point is C_1, as shown in Fig.10(a). After (8) is performed, the variable I_{2_min} is equal to 2.98A. The second peak needs to be checked, because I_{2_min} is lower than the short circuit current I_{sc} (4.0A). At $t = 1.15\,s$, the PV voltage is 57.4V, which is between V_{2_min} (44.24V) and V_{2_max} (60.04V), and the PV current is 2.78A. The operating point is switched to C_2. It is unnecessary to track the second peak because the I_i checking block in PSC MPPT subroutine is not met (I_{thres} is 0.1A, $|2.98A - 0.1A| > 2.78A$). And j is 2, therefore the

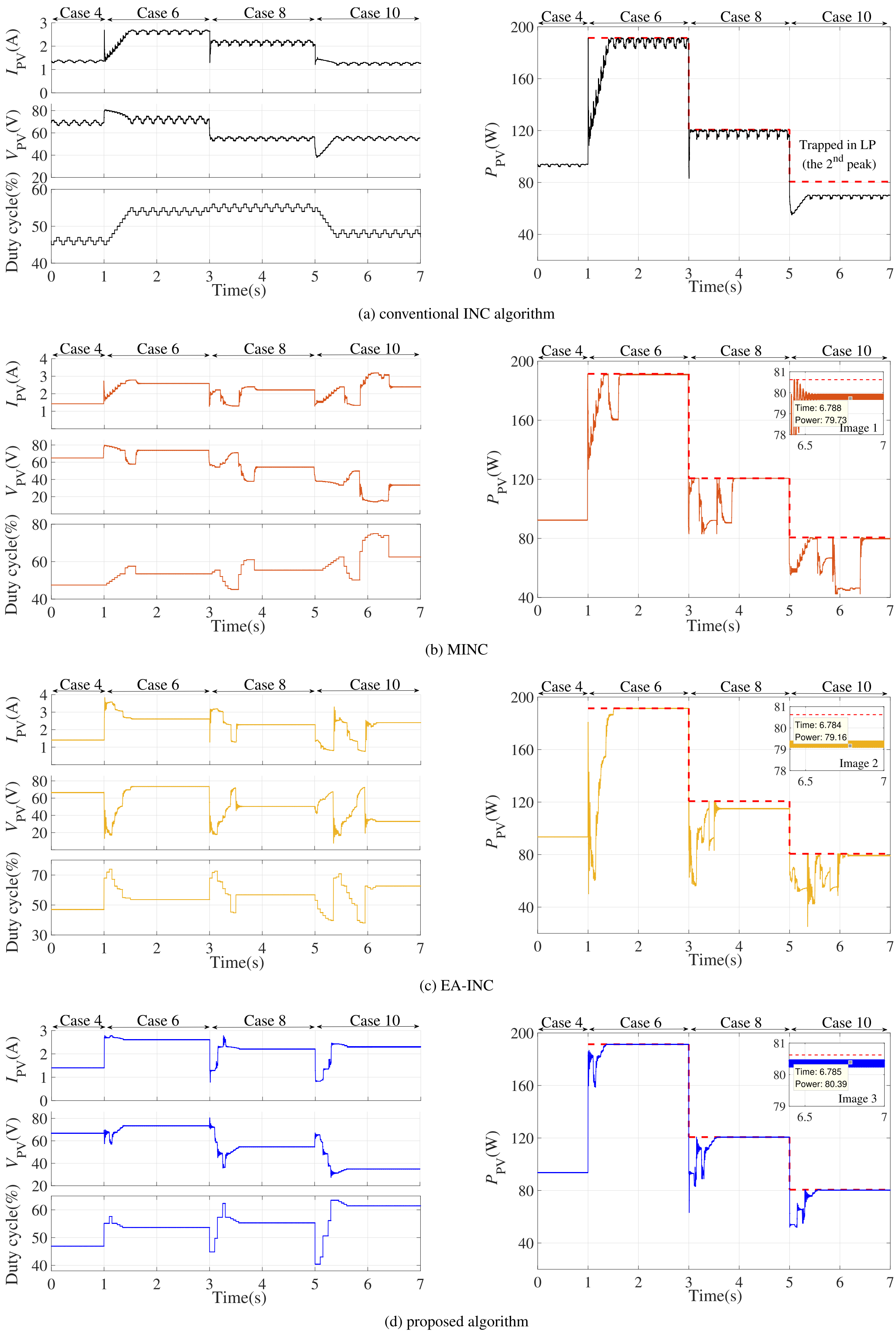

FIGURE 9. Simulation results of conventional INC, MINC, EA-INC and proposed algorithm under PSC.

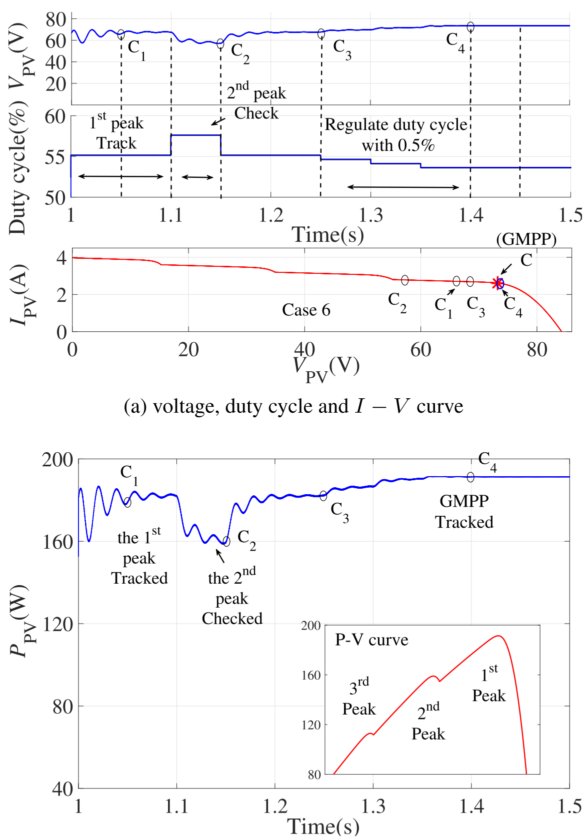

(a) voltage, duty cycle and $I-V$ curve

(b) power curve

FIGURE 10. The detialed tracking process of proposed method under case 6.

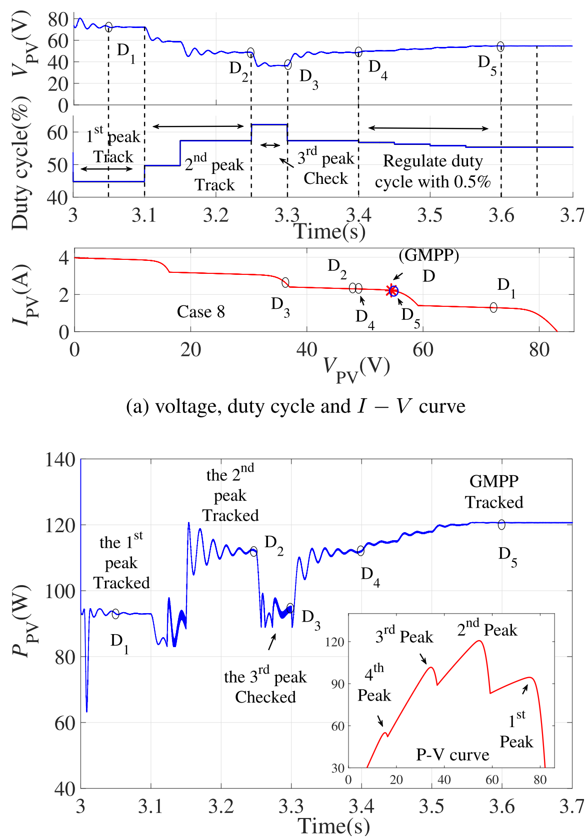

(a) voltage, duty cycle and $I-V$ curve

(b) power curve

FIGURE 11. The detialed tracking process of proposed method under case 8.

variable *Max_stage* is set to 1, that means the first peak is GP. From Fig.10(b), it can be found that the power of point C_2 is less than that of point C_1. So, the duty cycle is changed back to D_m. At $t = 1.25\,s$, since (7) is not satisfied, the duty cycle will be regulated with 0.5%. After 3 sampling cycles, $t = 1.40\,s$, the converter duty cycle is decreased to 53.64%, and (7) is satisfied. During the priod, the operating point is changed from C_3 to C_4, which comes in the vicinity of GP (point C). As can be seen from Fig.10(b), the tracked power is increased obviously from $t = 1.25\,s$ to $1.40\,s$.

2) GP AT THE SECOND PEAK

At $t = 3\,s$, the irradiance level is changed from case 6 to case 8. The conventional INC algorithm is the fastest method, which needs 1 sampling cycle to reach the GP. EA-INC and proposed method both take 0.6s. MINC requires 0.9s, and it is the slowest one. Although EA-INC is faster than MINC, its tracked power is less than that of other methods, as shown in Fig.9. Fig.11 presents the tracking process of the proposed method under case 8.

At $t = 3.05\,s$, the operating point is D_1, and (6) is satisfied, which means that the first peak is found. The PV power and duty cycle (93.05W and 44.82%) are saved as P_m and D_m, respectively. Since I_{2_min} (1.55A) is lower than I_{sc} (4.0A), the proposed method needs to check the second peak. At $t = 3.25\,s$, the power P_2 and duty cycle D_2 are 112.08W and 57.31%, respectively. Because P_2 is greater than P_m, the variables P_m and D_m are set to P_2 and D_2, respectively. After (8) is performed, the variable I_{3_min} is equal to 2.86A. At $t = 3.30\,s$, the PV voltage is 36.55V, which is between V_{3_min} (28.84V) and V_{3_max} (39.14V), the current I_3 is 2.56A, and the operating point is D_3. It is unnecessary to track the third peak because $(I_{3\_min} - 0.1) > I_3$ (i.e. the I_i checking block is not met). Then, the proposed algorithm determines if the fourth peak needs to be checked. According to (8), I_{4_min} is 6.14A, which is higher than I_{sc} (4.0A). So, there is no need to check the fourth peak. From $t = 3.40\,s$ to $3.60\,s$, the process that duty cycle is modulated slightly with 0.5% is performed, and the corresponding operating point is switched from D_4 to D_5, which reaches the vicinity of the GP (point D), as shown in Fig.11(a).

3) GP AT THE THIRD PEAK

At $t = 5\,s$, the irradiance level is switched to case 10. Except for the conventional INC method, other MPPT methods all can track the GP successfully, as presented in Fig.9. Under case 10, the conventional INC method is trapped in LP (the second peak). Among these algorithms, the proposed

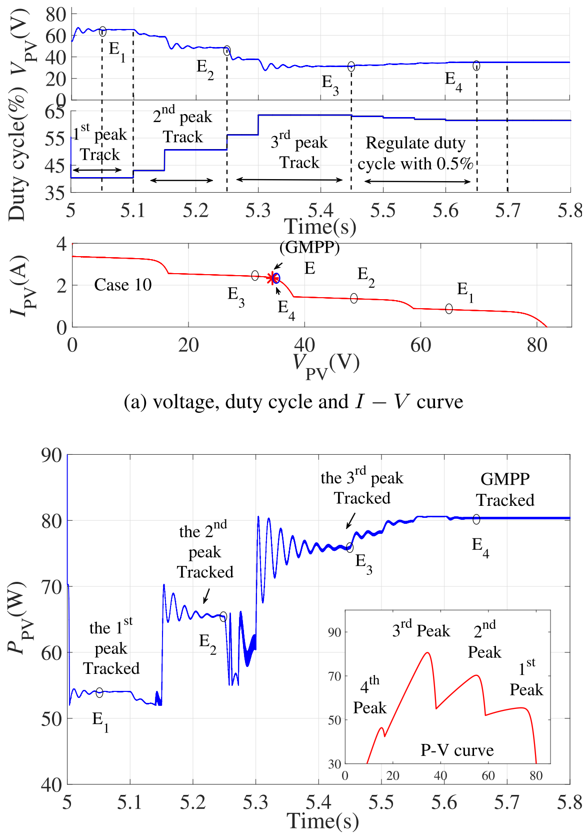

(a) voltage, duty cycle and $I - V$ curve

(b) power curve

FIGURE 12. The detialed tracking process of proposed method under case 10.

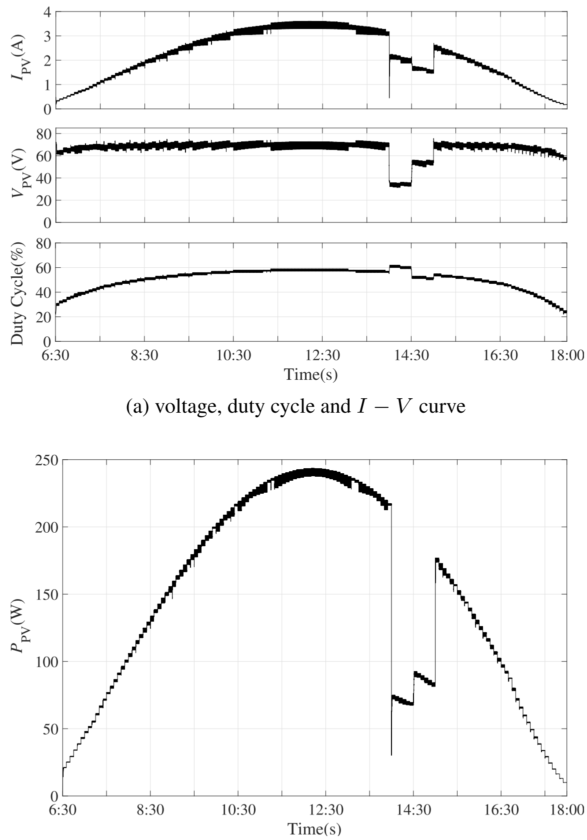

(a) voltage, duty cycle and $I - V$ curve

(b) power curve

FIGURE 13. Simulation results of conventional INC algorithm under one-day irradiance profile.

method exhibits shortest time (0.65s) to locate the GP. EA-INC and MINC need 1.2s and 1.5s, respectively. As can be found from images 1 to 3 in Fig.9, the power located by the proposed method is the highest, which is close to the theoretical available power (the red dotted line). The corresponding tracking process of the proposed method is sketched in Fig.12.

The proposed method locates the first peak at $t = 5.05\,s$, and the operating point is E_1, as shown in Fig.12. At $t = 5.25\,s$, the second peak is tracked, and the operating point is changed to E_2. At that time, the variables P_m and D_m are changed to 65.49W and 50.62%, respectively. After performing (8), I_{3_min} is 1.67A. At $t = 5.45\,s$, the third peak is located, and the operating point is switched to E_3. The PV voltage is 31.37V, which is between V_{3_min} (28.84V) and V_{3_max} (39.14V), the current I_3 is 2.43A. Since the third peak power P_3 is higher than P_m, the variables P_m and D_m are changed to 76.10W and 63.45%, respectively. The variable I_{4_min} is equal to 4.17A by using (8), and it is higher than I_{sc}. Thus, it is unnecessary to check the fourth peak. From $t = 5.45\,s$ to $5.65\,s$, the converter duty cycle is regulated with 0.5%, and the operating point is switched to E_4, which comes in the vicinity of the GP (point E), as presented in Fig.12(a). And the tracking efficiency is improved obviously, as shown in Fig.12(b).

C. TRACKING UNDER ONE-DAY IRRADIANCE PROFILE

Under this scenario, the 11.5-hour (6:30-18:00) irradiance profile of May 4, 2020, in Nanchang City, China, is applied. In order to simulate PSC case, the PV string is partially masked from $t = 14:00$ to $15:00$. At $14:00$, the shading factors of PV modules are 0, 0.3, 0.7 and 0.85 respectively, that means the PV modules receive 1 times, 0.7 times, 0.3 times, 0.15 times solar irradiance respectively. At $14:30$, the shading factors are changed to 0, 0.2, 0.5 and 0.4 respectively.

The conventional INC method and proposed algorithm are carried out, their initial duty cycle both are 25%, and the simulation results are shown in Fig.13 and Fig.14. Under UIC, these methods all can locate the GP, but the conventional INC method has larger steady state oscillation than the proposed algorithm. While the oscillation of proposed method is neglected because of the use of (6) and (7). From $t = 14:00$ to $14:30$, PSC occurs, and GP is positioned at the third peak. These methods can track the GP successfully, but the proposed method has larger power losses, compared to conventional INC. From $t = 14:30$ to $15:00$, the GP is located at the first peak (rightmost peak), and it can be found that only the proposed method can track the GP successfully. While the conventional INC is trapped in LP (the second peak), as shown in the voltage wave of conventional INC

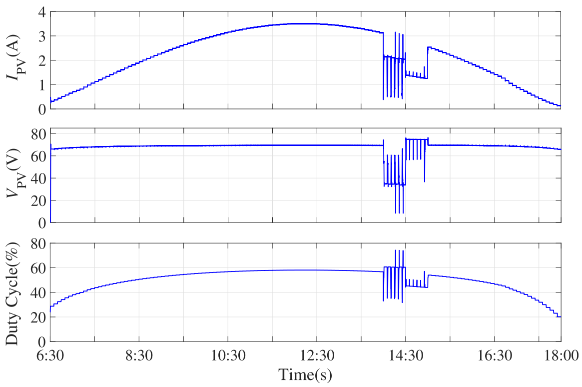

(a) voltage, duty cycle and $I - V$ curve

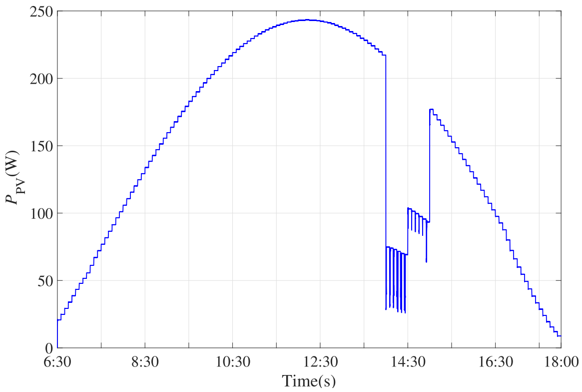

(b) power curve

FIGURE 14. Simulation results of proposed algorithm under one-day irradiance profile.

TABLE 4. Simulation results comparision under UIC and one-day irradiance profile.

Scenario	Tracking time (s)		Efficiency (%)	
	INC	Proposed	INC	Proposed
Case 1	0.65	0.15	83.34	99.71
Case 2	0.60	0.10	85.36	99.83
Case 5	0.90	0.10	71.73	99.53
Load increase	0.50	0.15	92.52	98.63
Load decrease	0.40	0.20	94.59	97.90
One day			98.78	99.20

method. Although the proposed method causes larger power losses than conventional INC under PSC, it can track the GP sucessfully.

D. EVALUATION

Tables 4 and 5 show the simluation results comparision such as the tracking time and efficiency. It is noted that the performance of the first 1s for case 4 is not taken into account in the performance evaluation.

Table 4 shows the results comparison under UIC and one-day irradiance profile. As can be found from Table 4, the proposed method (0.12s and 99.69%) is faster and more efficient than conventional INC (0.72s and 80.14%), for the irradiance variation condition. Under the load variation scenario, the proposed method (98.27% and 0.18s) is still better than conventional INC (93.56% and 0.45s). So, the converging speed with the proposed algorithm is 4.36 times faster than that of conventional INC, and the efficiency is increased by 13.61%, under UIC. For the efficiency of one-day irradiance profile, the proposed method is 99.20%, which is 0.42% higher than the conventional INC.

TABLE 5. Simulation results comparision under PSC.

Scenario	Tracking time (s)				Efficiency (%)			
	INC	MINC	EA-INC	Proposed	INC	MINC	EA-INC	Proposed
Case 6	0.50	0.65	0.55	0.40	94.15	95.26	87.57	98.82
Case 8	0.05	0.90	0.60	0.60	98.41	90.87	89.89	96.52
Case 10		1.50	1.20	0.65	84.48	81.95	83.14	94.56

The results comparison under PSC is given in Table 5. It can be found that the proposed algorithm is the fastest one under many cases, except for case 8. Although the converging speed with conventional INC is faster than other methods under case 8, it can not locate the GP under case 10. In term of overall tracking time, the proposed method requires 0.55s to track the GP, EA-INC and MINC take 0.78s and 1.02s, respectively. Among these MPPT methods, the proposed method is the most efficient one, at 96.63%. While the conventional INC and MINC are 92.35% and 89.36%, respectively. The lowest one is EA-INC, which is 86.87%. So, the proposed method is hte best one, and it can track the GP fast and efficiently under both UIC and PSC.

V. CONCLUSIONS

In this work, a modified INC method is proposed to locate the GP under both UIC and PSC. This algorithm can not only distinguish between the irradiance variation under UIC and the occurrence of PSC, but also determine if the other peaks need to be tracked under PSC, by using the relationship between the minimum current at other peaks and the short circuit current. In order to improve the tracking efficiency, the converter duty cycle can be regulated slightly after the approximate GP location is found, which makes sure the operating point is positioned in the vicinity of GP. Different scenarios such as the UIC case, PSC case and one-day irradiance profile are analyzed. The results show the proposed method is faster and more efficient than other methods. And it only needs 0.14s (about 3 sample cycles) and 0.55s (11 sample cycles) to track the GP under UIC and PSC, respectively. In addition, the overall tracking efficiency with the proposed method is increased by 13.61% and 4.28% under UIC and PSC respectively, compared to the conventional INC algorithm.

REFERENCES

[1] S. Motahhir, A. El Ghzizal, S. Sebti, and A. Derouich, "Modeling of photovoltaic system with modified incremental conductance algorithm for fast changes of irradiance," *Int. J. Photoenergy*, vol. 2018, Mar. 2018, Art. no. 3286479.

[2] K. S. Tey and S. Mekhilef, "Modified incremental conductance MPPT algorithm to mitigate inaccurate responses under fast-changing solar irradiation level," *Sol. Energy*, vol. 101, pp. 333–342, Mar. 2014.

[3] N. Kumar, I. Hussain, B. Singh, and B. K. Panigrahi, "Self-adaptive incremental conductance algorithm for swift and ripple-free maximum power harvesting from PV array," *IEEE Trans. Ind. Informat.*, vol. 14, no. 5, pp. 2031–2041, May 2018.

[4] D. Verma, S. Nema, A. M. Shandilya, and S. K. Dash, "Maximum power point tracking (MPPT) techniques: Recapitulation in solar photovoltaic systems," *Renew. Sustain. Energy Rev.*, vol. 54, pp. 1018–1034, Feb. 2016.

[5] M. F. N. Tajuddin, M. S. Arif, S. M. Ayob, and Z. Salam, "Perturbative methods for maximum power point tracking (MPPT) of photovoltaic (PV) systems: A review," *Int. J. Energy Res.*, vol. 39, no. 9, pp. 1153–1178, Jul. 2015.

[6] Z. Salam, J. Ahmed, and B. S. Merugu, "The application of soft computing methods for MPPT of PV system: A technological and status review," *Appl. Energy*, vol. 107, pp. 135–148, Jul. 2013.

[7] M. Killi and S. Samanta, "Modified perturb and observe MPPT algorithm for drift avoidance in photovoltaic systems," *IEEE Trans. Ind. Electron.*, vol. 62, no. 9, pp. 5549–5559, Sep. 2015.

[8] Q. Duan, J. Leng, P. Duan, B. Hu, and M. Mao, "An improved variable step PO and global scanning MPPT method for PV systems under partial shading condition," in *Proc. 7th Int. Conf. Intell. Hum.-Mach. Syst. Cybern.*, Aug. 2015, pp. 382–386.

[9] K. S. Tey, S. Mekhilef, M. Seyedmahmoudian, B. Horan, A. T. Oo, and A. Stojcevski, "Improved differential evolution-based MPPT algorithm using SEPIC for PV systems under partial shading conditions and load variation," *IEEE Trans. Ind. Informat.*, vol. 14, no. 10, pp. 4322–4333, Oct. 2018.

[10] Y.-H. Liu, C.-L. Liu, J.-W. Huang, and J.-H. Chen, "Neural-network-based maximum power point tracking methods for photovoltaic systems operating under fast changing environments," *Sol. Energy*, vol. 89, pp. 42–53, Mar. 2013.

[11] L. M. Elobaid, A. K. Abdelsalam, and E. E. Zakzouk, "Artificial neural network-based photovoltaic maximum power point tracking techniques: A survey," *IET Renew. Power Gener.*, vol. 9, no. 8, pp. 1043–1063, Nov. 2015.

[12] K. Punitha, D. Devaraj, and S. Sakthivel, "Artificial neural network based modified incremental conductance algorithm for maximum power point tracking in photovoltaic system under partial shading conditions," *Energy*, vol. 62, pp. 330–340, Dec. 2013.

[13] K. Kaced, C. Larbes, N. Ramzan, M. Bounabi, and Z. E. Dahmane, "Bat algorithm based maximum power point tracking for photovoltaic system under partial shading conditions," *Sol. Energy*, vol. 158, pp. 490–503, Dec. 2017.

[14] M. Kermadi and E. M. Berkouk, "Artificial intelligence-based maximum power point tracking controllers for photovoltaic systems: Comparative study," *Renew. Sustain. Energy Rev.*, vol. 69, pp. 369–386, Mar. 2017.

[15] D. Yousri, T. S. Babu, D. Allam, V. K. Ramachandaramurthy, E. Beshr, and M. B. Eteiba, "Fractional chaos maps with flower pollination algorithm for partial shading mitigation of photovoltaic systems," *Energies*, vol. 12, no. 18, p. 3548, Sep. 2019.

[16] K. Ishaque, Z. Salam, M. Amjad, and S. Mekhilef, "An improved particle swarm optimization (PSO)–based MPPT for PV with reduced steady-state oscillation," *IEEE Trans. Power Electron.*, vol. 27, no. 8, pp. 3627–3638, Aug. 2012.

[17] D. Yousri, T. S. Babu, D. Allam, V. K. Ramachandaramurthy, and M. B. Etiba, "A novel chaotic flower pollination algorithm for global maximum power point tracking for photovoltaic system under partial shading conditions," *IEEE Access*, vol. 7, pp. 121432–121445, 2019.

[18] K. Hu, S. Cao, W. Li, and F. Zhu, "An improved particle swarm optimization algorithm suitable for photovoltaic power tracking under partial shading conditions," *IEEE Access*, vol. 7, pp. 143217–143232, 2019.

[19] H. Patel and V. Agarwal, "Maximum power point tracking scheme for PV systems operating under partially shaded conditions," *IEEE Trans. Ind. Electron.*, vol. 55, no. 4, pp. 1689–1698, Apr. 2008.

[20] K. Chen, S. Tian, Y. Cheng, and L. Bai, "An improved MPPT controller for photovoltaic system under partial shading condition," *IEEE Trans. Sustain. Energy*, vol. 5, no. 3, pp. 978–985, Jul. 2014.

[21] K. Soon Tey and S. Mekhilef, "Modified incremental conductance algorithm for photovoltaic system under partial shading conditions and load variation," *IEEE Trans. Ind. Electron.*, vol. 61, no. 10, pp. 5384–5392, Oct. 2014.

[22] J. Ahmed and Z. Salam, "An enhanced adaptive P&O MPPT for fast and efficient tracking under varying environmental conditions," *IEEE Trans. Sustain. Energy*, vol. 9, no. 3, pp. 1487–1496, Jul. 2018.

[23] M. A. Ghasemi, H. M. Foroushani, and M. Parniani, "Partial shading detection and smooth maximum power point tracking of PV arrays under PSC," *IEEE Trans. Power Electron.*, vol. 31, no. 9, pp. 6281–6292, Sep. 2016.

[24] C. Manickam, G. R. Raman, G. P. Raman, S. I. Ganesan, and C. Nagamani, "A hybrid algorithm for tracking of GMPP based on P&O and PSO with reduced power oscillation in string inverters," *IEEE Trans. Ind. Electron.*, vol. 63, no. 10, pp. 6097–6106, Oct. 2016.

[25] Z. Erdem, "A review of MPPT algorithms for partial shading conditions," *Acta Phys. Polonica A*, vol. 132, no. 3, pp. 1128–1133, Sep. 2017.

[26] S. Mohanty, B. Subudhi, and P. K. Ray, "A grey wolf-assisted perturb & observe MPPT algorithm for a PV system," *IEEE Trans. Energy Convers.*, vol. 32, no. 1, pp. 340–347, Mar. 2017.

[27] W. Zhang, G. Zhou, H. Ni, and Y. Sun, "A modified hybrid maximum power point tracking method for photovoltaic arrays under partially shading condition," *IEEE Access*, vol. 7, pp. 160091–160100, 2019.

[28] Y. Wang, Y. Li, and X. Ruan, "High-accuracy and fast-speed MPPT methods for PV string under partially shaded conditions," *IEEE Trans. Ind. Electron.*, vol. 63, no. 1, pp. 235–245, Jan. 2016.

[29] D. Wei, Y. Chang, J. Zang, H. Cai, and H. Zhou, "Multimodal MPPT algorithm for series PV modules based on linear equation and peak partial PV module," *Acta Energiae Sol. Sin.*, vol. 41, no. 1, pp. 125–131, 2020.

[30] R. Fan, G. Yin, J. Miao, and D. Xie, "A quick MPPT method of PV panel based on parameter identification," *Acta Energiae Sol. Sin.*, vol. 41, no. 2, pp. 296–302, 2020.

[31] *Solarex MSX-60 and MSX-64 Photovoltaic Modules Datasheet*. [Online]. Available: https://www.solarelectricsupply.com/media/custom/upload/Solarex-MSX64.pdf

[32] R. F. Coelho, F. Concer, and D. C. Martins, "A study of the basic DC-DC converters applied in maximum power point tracking," in *Proc. Brazilian Power Electron. Conf.*, Bonito-Mato Grosso do Sul, Brazil, Sep. 2009, pp. 673–678.

[33] R. W. Erickson and D. Maksimovic, *Fundamentals of Power Electronics*. New York, NY, USA: Springer, 2007, pp. 16–31.

[34] T. K. Soon and S. Mekhilef, "A fast-converging MPPT technique for photovoltaic system under fast-varying solar irradiation and load resistance," *IEEE Trans. Ind. Informat.*, vol. 11, no. 1, pp. 176–186, Feb. 2015.

[35] L. Xu, R. Cheng, and J. Yang, "A new MPPT technique for fast and efficient tracking under fast varying solar irradiation and load resistance," *Int. J. Photoenergy*, vol. 2020, pp. 1–18, Feb. 2020.

LIBIN XU was born in Guangdong, China, in 1995. He received the B.S. degree in automation from Shao Yang University, China, in 2018. He is currently pursuing the M.Sc. degree in control engineering with Nanchang Hangkong University, China.

His current research interests include photovoltaic control and power efficiency of PV systems.

RUOFA CHENG was born in Anhui, China, in 1972. He received the Ph.D. degree in control engineering from the Graduate University of Chinese Academy of Sciences, Beijing, China, in 2008.

He is currently an Associate Professor with the School of Information Engineering, Nanchang Hangkong University. His research interests include smart grids, energy management, power systems operation, demand response, electricity markets, renewable energy sources, and energy efficiency.

JIAJING YANG was born in Shaanxi, China, in 1996. She received the B.S. degree in measurement-control technology and instrumentation from Liao Dong University, China, in 2018. She is currently pursuing the M.Sc. degree in control engineering with Nanchang Hangkong University, China.

Her research interests include distributed generation and renewable energy generation.